Hexanuclear Arene Clusters of Ruthenium†

Paul J. Dyson,[a] Brian F. G. Johnson,*[,a] David Reed,[a] Dario Braga,*[b] Fabrizia Grepioni[b] and Emilio Parisini[b]

[a] *Department of Chemistry, University of Edinburgh, West Mains Road, Edinburgh EH9 3JJ, UK*

[b] *Dipartimento di Chimica G. Ciamician, Università di Bologna, Via Selmi 2, 40126 Bologna, Italy*

The hexanuclear cluster $[Ru_6C(CO)_{14}(\eta^6\text{-arene})]$ **1** (arene = C_6H_6, C_6H_5Me, $C_6H_4Me_2$-1,3 or $C_6H_3Me_3$-1,3,5) reacts with Me_3NO–CH_2Cl_2 in the presence of cyclohexa-1,3-diene or cyclohexa-1,4-diene to yield compound $[Ru_6C(CO)_{12}(\eta^6\text{-arene})(\mu\text{-}\eta^2\text{:}\eta^2\text{-}C_6H_8)]$ **2** in which the diene spans one metal edge of the octahedral cluster unit. Further treatment of **2** with Me_3NO–CH_2Cl_2 affords the bis(arene) derivative $[Ru_6C(CO)_{11}(\eta^6\text{-arene})(C_6H_6)]$. On the basis of spectroscopic data and single-crystal X-ray data it appears that these bis(arene) derivatives exist in two isomeric forms, *viz.* $[Ru_6C(CO)_{11}(\eta^6\text{-arene})(\mu_3\text{-}\eta^2\text{:}\eta^2\text{:}\eta^2\text{-}C_6H_6)]$ **3** and $[Ru_6C(CO)_{11}(\eta^6\text{-arene})(\eta^6\text{-}C_6H_6)]$ **4**. Evidence that compound **3** is formed initially, followed by isomerisation to **4** is presented. The structures of $[Ru_6C(CO)_{11}(\eta^6\text{-}C_6H_5Me)(\mu_3\text{-}\eta^2\text{:}\eta^2\text{:}\eta^2\text{-}C_6H_6)]$ **3b** and $[Ru_6C(CO)_{11}(\eta^6\text{-}C_6H_4Me_2\text{-}1,3)(\mu_3\text{-}\eta^2\text{:}\eta^2\text{:}\eta^2\text{-}C_6H_6)]$ **3c** have been determined by single-crystal X-ray diffraction. Compound **3b** is orthorhombic, space group *Pnma*, $a = 9.035(5)$, $b = 14.796(2)$, $c = 20.534(4)$ Å, $Z = 4$, 1770 unique observed reflections $[I > 2\sigma(I)]$, $R = 0.020$; **3c** is monoclinic, space group $P2_1/n$, $a = 18.27(2)$, $b = 9.729(2)$, $c = 34.39(3)$ Å, $\beta = 94.94(6)°$, $Z = 8$, 7833 unique observed reflections $[I > 2.0\sigma(I)]$, $R = 0.058$, $R' = 0.062$.

During the course of our studies we have prepared and structurally characterised a wide variety of ruthenium and osmium clusters in which arenes are incorporated as ligands. Amongst the earliest examples of arene-cluster compounds were the hexaruthenium–carbido clusters, $[Ru_6C(CO)_{14}(\eta^6\text{-arene})]$ (arene = C_6H_6, C_6H_5Me, $C_6H_4Me_2$-1,3 or $C_6H_3Me_3$-1,3,5),[1–3] prepared by heating $[Ru_3(CO)_{12}]$ with the respective arene. The η^6-co-ordination mode of the arene ligand was confirmed by a single-crystal X-ray diffraction study of the mesitylene derivative,[4] and later for the toluene species.[5] The η^6-bonding mode has also been observed in M_3 (M = Ru[6] or Os[6,7]), M_4 (M = Ru[8] or Os[9]), and Ru_5 clusters.[10,11] The η^6-co-ordination mode for arenes, although predominant, is not unique to ruthenium and osmium clusters.

An alternative type of co-ordination mode for benzene was discovered in the compounds $[Os_3(CO)_9(\mu_3\text{-}\eta^2\text{:}\eta^2\text{:}\eta^2\text{-}C_6H_6)]$ and $[Ru_6C(CO)_{11}(\eta^6\text{-}C_6H_6)(\mu_3\text{-}\eta^2\text{:}\eta^2\text{:}\eta^2\text{-}C_6H_6)]$,[12] in which the ring is symmetrically bonded over the face of a metal triangle. This face-capping co-ordination of benzene has since been found in Ru_3[13,14] and Ru_5 clusters.[10] This co-ordination mode accurately models the non-dissociative chemisorption of benzene at surface metal atoms in low Miller index planes of close-packed arrays of a metallic lattice.[15] Of equal interest is the observation that the face-capping benzene may undergo migration to a single metal site within the cluster. This has been achieved chemically in $[M_3(CO)_9(\mu_3\text{-}\eta^2\text{:}\eta^2\text{:}\eta^2\text{-}C_6H_6)]$ (M = Ru or Os[6,7]) upon reaction of the clusters with acetylenes. In $[Ru_5C(CO)_{12}(\mu_3\text{-}\eta^2\text{:}\eta^2\text{:}\eta^2\text{-}C_6H_6)]$ the migration of the benzene moiety from the face-capping mode has been brought about by thermolysis to afford $[Ru_5C(CO)_{12}(\eta^6\text{-}C_6H_6)]$, in which the benzene ligand co-ordinates to a ruthenium atom on the base of the square-pyramidal metal framework.[11] The migration of benzene in $[Ru_6C(CO)_{11}(\eta^6\text{-}C_6H_3Me_3\text{-}1,3,5)(\mu_3\text{-}\eta^2\text{:}\eta^2\text{:}\eta^2\text{-}C_6H_6)]$ to a metal *cis* to the ruthenium atom to which the mesitylene co-ordinates, resulting in $[Ru_6C(CO)_{11}(\eta^6\text{-}C_6H_3Me_3\text{-}1,3,5)(\eta^6\text{-}C_6H_6)]$ has been found to be reversible.[16]

In this report we demonstrate that the phenomenon of η^6-/μ_3-η^2:η^2:η^2-benzene interconversion is not isolated to the above example, but the reversible isomerisation also manifests itself in the clusters $[Ru_6C(CO)_{11}(\eta^6\text{-arene})(C_6H_6)]$ (arene = C_6H_6, C_6H_5Me or $C_6H_4Me_2$-1,3).

Results and Discussion

Synthesis and Chemical Characterisation.—Recently we demonstrated that the cluster dianion $[Ru_5C(CO)_{14}]^{2-}$ undergoes reaction with the dication $[Ru(C_6H_6)(MeCN)_3]^{2+}$ to produce the benzene cluster derivative $[Ru_6C(CO)_{14}(\eta^6\text{-}C_6H_6)]$ **1a** in high yield;[12] this is also a minor product from the direct reaction of $[Ru_3(CO)_{12}]$ with benzene.[3] We find that these ionic coupling reactions are general and may be applied to generate the range of hexaruthenium–arene clusters $[Ru_6C(CO)_{14}(\eta^6\text{-arene})]$ (arene = C_6H_5Me **1b**, $C_6H_4Me_2$-1,3 **1c** or $C_6H_3Me_3$-1,3,5 **1d**) (Scheme 1). These compounds have also been reported as the products of the direct reaction of $[Ru_3(CO)_{12}]$ with the appropriate arene.[1,2]

The reaction of $[Ru_6(C(CO)_{14}(\eta^6\text{-arene})]$ **1** with 2 molecular equivalents of trimethylamine *N*-oxide (Me_3NO) in CH_2Cl_2 in the presence of cyclohexa-1,3-diene or cyclohexa-1,4-diene affords, as the major product, $[Ru_6C(CO)_{12}(\eta^6\text{-arene})(\mu\text{-}\eta^2\text{:}\eta^2\text{-}C_6H_8)]$ (arene = C_6H_6 **2a**, C_6H_5Me **2b**, $C_6H_4Me_2$-1,3 **2c** or $C_6H_3Me_3$-1,3,5 **2d**), and as a minor product the bis(arene) compounds $[Ru_6C(CO)_{11}(\eta^6\text{-arene})(\mu_3\text{-}\eta^2\text{:}\eta^2\text{:}\eta^2\text{-}C_6H_6)]$ (arene = C_6H_6 **3a**, C_6H_5Me **3b**, $C_6H_4Me_2$-1,3 **3c** or $C_6H_3Me_3$-1,3,5 **3d**). An isomeric form of **3a**, namely $[Ru_6C(CO)_{11}(\eta^6\text{-}C_6H_6)_2]$ in which the two benzene moieties 'sandwich' the metal cluster has been obtained recently.[17] In compounds **2a**–**2d** the diene co-ordinates in the 1,3-form regardless of the diene used in the reaction. Although the mechanism of the isomerisation of cyclohexa-1,4-diene to cyclohexa-1,3-diene, upon co-ordination, is not fully understood, it is not unexpected and is similar to the behaviour observed in the formation of cyclohexa-1,3-diene derivatives of the mononuclear unit $M(CO)_3$ (M = Fe, Ru or Os). In turn, clusters **2a**–**2d** react with a further equivalent

† *Supplementary data available:* see Instructions for Authors, *J. Chem. Soc., Dalton Trans.*, 1993, Issue 1, pp. xxiii–xxviii.

Table 1 Infrared and mass spectroscopic data for compounds **2–4**

Compound	$\tilde{\nu}$/cm^{-1}	*m/z* *
2a $[Ru_6C(CO)_{12}(\eta^6\text{-}C_6H_6)(\mu\text{-}\eta^2\text{:}\eta^2\text{-}C_6H_8]$	2044m, 2001vs, 1966w, 1821w (br)	1113 (1113)
2b $[Ru_6C(CO)_{12}(\eta^6\text{-}C_6H_5Me)(\mu\text{-}\eta^2\text{:}\eta^2\text{-}C_6H_8)]$	2043m, 2000vs, 1967w, 1818w (br)	1128 (1127)
2c $[Ru_6C(CO)_{12}(\eta^6\text{-}C_6H_4Me_2\text{-}1,3)(\mu\text{-}\eta^2\text{:}\eta^2\text{-}C_6H_8]$	2042m, 1999vs, 1964w, 1820w (br)	1142 (1141)
2d $[Ru_6C(CO)_{12}(\eta^6\text{-}C_6H_3Me_3\text{-}1,3,5)(\mu\text{-}\eta^2\text{:}\eta^2\text{-}C_6H_8)]$	2041m, 1998vs, 1964w, 1814w (br)	1155 (1155)
3a $[Ru_6C(CO)_{11}(\eta^6\text{-}C_6H_6)(\mu_3\text{-}\eta^2\text{:}\eta^2\text{:}\eta^2\text{-}C_6H_6)]$	2039m, 2002vs, 1950w, 1800w (br)	1084 (1083)
3b $[Ru_6C(CO)_{11}(\eta^6\text{-}C_6H_5Me)(\mu_3\text{-}\eta^2\text{:}\eta^2\text{:}\eta^2\text{-}C_6H_6)]$	2038m, 2001vs, 1950w, 1797w (br)	1098 (1097)
3c $[Ru_6C(CO)_{11}(\eta^6\text{-}C_6H_4Me_2\text{-}1,3)(\mu_3\text{-}\eta^2\text{:}\eta^2\text{:}\eta^2\text{-}C_6H_6)]$	2037m, 2000vs, 1947w, 1997w (br)	1112 (1111)
3d $[Ru_6C(CO)_{11}(\eta^6\text{-}C_6H_3Me_3\text{-}1,3,5)(\mu_3\text{-}\eta^2\text{:}\eta^2\text{:}\eta^2\text{-}C_6H_6)]$	2037m, 1999vs, 1944w, 1793w (br)	1126 (1125)
4a $[Ru_6C(CO)_{11}(\eta^6\text{-}C_6H_6)(\eta^6\text{-}C_6H_6)]$	2052m, 2001vs, 1949w, 1800w (br)	
4b $[Ru_6C(CO)_{11}(\eta^6\text{-}C_6H_5Me)(\eta^6\text{-}C_6H_6)]$	2051m, 2000vs, 1950w, 1796w (br)	
4c $[Ru_6C(CO)_{11}(\eta^6\text{-}C_6H_4Me_2\text{-}1,3)(\eta^6\text{-}C_6H_6)]$	2050m, 1999vs, 1947w, 1796w (br)	
4d $[Ru_6C(CO)_{11}(\eta^6\text{-}C_6H_3Me_3\text{-}1,3,5)(\eta^6\text{-}C_6H_6)]$	2048m, 1996vs, 1948w, 1792w (br)	1126 (1125)

* Calculated values given in parentheses.

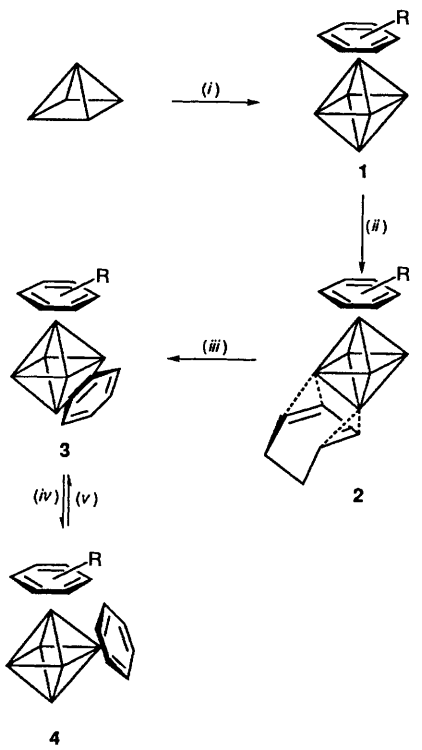

Scheme 1 The synthesis of bis(arene) hexanuclear clusters from $[Ru_5C(CO)_{15}]$. Reagents and conditions: (*i*) addition of $[Ru_5C(CO)_{14}]^{2-}$ into a refluxing solution of $[Ru(arene)(MeCN)_3]^{2+}$ (arene = C_6H_6, C_6H_5Me, $C_6H_4Me_2$-1,3 or $C_6H_3Me_3$-1,3,5); (*ii*) Me_3NO–CH_2Cl_2 added dropwise to a solution of **1** in CH_2Cl_2–C_6H_8-1,3; (*iii*) Me_3NO–CH_2Cl_2 added dropwise to a solution of **2** in CH_2Cl_2; (*iv*) standing of a CH_2Cl_2 solution of **3** at −25 °C for a prolonged period; (*v*) refluxing of **4** in hexane for a few hours

of Me_3NO in CH_2Cl_2 to generate the clusters **3a–3d**, thus improving the overall yield. This reaction presumably occurs first by the oxidative removal of one CO ligand to CO_2 to produce the co-ordinatively unsaturated derivative of the type $[Ru_6C(CO)_{11}(arene)(C_6H_8)]$, which then undergoes 'dehydrogenation' of the C_6H_8 ring, hence affording the arene–benzene cluster.

On standing at −25 °C in CH_2Cl_2 for a prolonged period, infrared spectroscopy indicates that compounds **3a–3d** undergo conversion to afford the new isomers $[Ru_6C(CO)_{11}(\eta^6\text{-arene})(\eta^6\text{-}C_6H_6)]$ (arene = C_6H_6 **4a**, C_6H_5Me **4b**, $C_6H_4Me_2$-1,3 **4c** or $C_6H_3Me_3$-1,3,5 **4d**) in which the C_6 aromatic rings bind to ruthenium atoms *cis* to one another on the cluster framework. The ease of isomerisation occurs according to the series **3d** > **3c** > **3b** > **3a**. These new isomers may be converted back to their original form **3a–3d** by heating in hexane for several hours.

All the compounds **2a–2d** exhibit a similar IR spectrum in the ν_{CO} region (Table 1). The symmetry of the spectrum remains virtually unchanged upon alteration of the arene, while the main stretches decrease in wavenumber by approximately 1 cm^{-1} for each methyl group substituted on to the aromatic ring. The ^{1}H NMR spectra of compounds **2a–2d** are also similar to one another. The signals deriving from the diene moiety are typical for the whole series and, in this instance, are labelled A–H, as shown in Fig. 1. The signals at δ 4.95, 4.90, 4.26 and 3.53 are consistent with the 'olefinic' protons of the diene system, while those at δ 2.10, 1.97, 1.00 and 0.83 arise from the 'aliphatic' protons of the diene. The proton homonuclear two-dimensional correlation spectroscopy (COSY) plot of the region (also illustrated in Fig. 1) shows correlation linking H/F, H/C, G/E and G/D, suggesting that the signals arising from G and H derive from the 1 and 4 positions on the diene. Signals E and F can therefore be ascribed to positions 2 and 3.

The chemical shift values of signals E and F are quite unusual for protons on a double bond, suggesting that carbon atoms C^2 and C^3 are those most strongly associated with the metal core. The relative stereochemistries of the protons giving rise to signals A–D, which are located on carbon atoms C^5 and C^6, can be speculated on the basis of both chemical shift and nuclear Overhauser effect (NOE) evidence. The NOE data are summarised in Table 2. The fact that eight signals are observed for the diene, along with the range of chemical shifts, suggests that the diene is bound asymmetrically to the octahedral metal core. This observation is consistent with the gross structural features obtained from the single-crystal X-ray analysis of **2b** which is not reported due to the poor quality of the data, and that of $[Ru_6C(CO)_{12}(\eta^6\text{-}C_6H_6)(\mu\text{-}\eta^2\text{:}\eta^2\text{-}C_6H_8)]$ **2a** reported elsewhere.[18]

The remaining signals obtained in the ^{1}H NMR spectra of **2a–2d** are summarised in Table 3. Particularly noteworthy are the spectra of **2b** and **2c**. The spectrum of **2b** shows five different aromatic toluene signals, consistent with the asymmetry inherent in the system. Similarly, two methyl signals are obtained for **2c**.

Similarly, the IR spectra of compounds **3a–3d** in the ν_{CO} region (Table 1) are closely related. While the overall symmetry remains the same, the shift of the spectra to lower wavenumber with increasing methyl group substitution on the aromatic ring is apparent. Their ^{1}H NMR spectra are much simpler than those of **2a–2d**, and also are summarised in Table 3.

Particularly characteristic are the shifts of the arene protons. Where η^6 bonding is found, the chemical shifts of the protons are *ca.* δ 5.5, whereas for the $\mu_3\text{-}\eta^2\text{:}\eta^2\text{:}\eta^2$-co-ordinated benzene groups, the proton chemical shift values are *ca.* δ 4.1.

The bis(terminal) mesitylene–benzene cluster **4d** has previously been reported;[16] it was fully characterised by spectroscopic methods (see Table 1) and also in the solid state

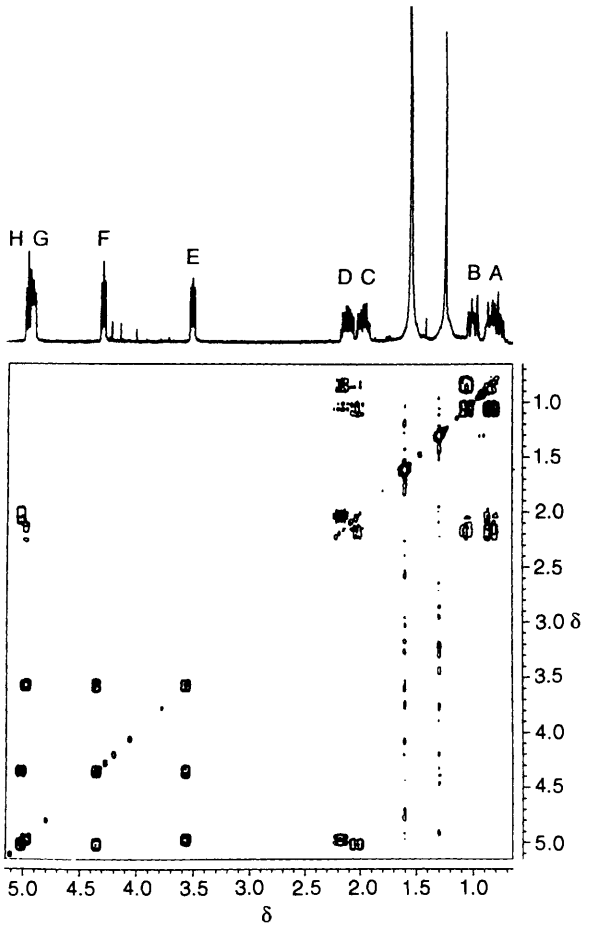

Fig. 1 The ^{1}H NMR and COSY spectra showing the signals derived from the cyclohexa-1,3-diene moiety of $[Ru_6C(CO)_{12}(\eta^6\text{-}C_6H_6)(\mu\text{-}\eta^2\text{:}\eta^2\text{-}C_6H_8)]$ **2a**

by single-crystal X-ray diffraction. It was found that the two arenes co-ordinate to ruthenium atoms which are *cis* to one another on the octahedral metal framework. The remaining species in this series, **4a**–**4c**, have been characterised on the basis of the characteristic IR spectra produced in the ν_{CO} region (Table 1).

Molecular Structures of $[Ru_6C(CO)_{11}(\eta^6\text{-arene})(\mu_3\text{-}\eta^2\text{:}\eta^2\text{:}\eta^2\text{-}C_6H_6)]$ (*arene* = C_6H_5Me **3b** *or* $C_6H_4Me_2$-1,3 **3c**).—The molecular structures of **3b** and **3c** are closely related and will be discussed together. Molecular sketches are shown in Figs. 2 and 3 for **3b** and **3c**, respectively. Note that only one of the two crystallographically independent molecules present in the asymmetric unit of **3c** is shown (see below). Relevant structural parameters for **3b** and **3c** are listed in Tables 4 and 5, respectively. Both complexes possess the familiar hexaruthenium cluster core present in $[Ru_6C(CO)_{17}]$,[19] and its derivatives, the octahedral cavity accommodating the interstitial C(carbide) atom. The two complexes are characterised by the presence of two arene ligands bound to the metal frame. In both **3b** and **3c** the methyl substituted ligand is in an apical position (η^6-bonding mode) while the benzene ligand is bound in face-capping ($\mu_3\text{-}\eta^2\text{:}\eta^2\text{:}\eta^2$) bonding mode. The distribution of the arene ligands is thus similar to that observed previously in $[Ru_6C(CO)_{11}(\eta^6\text{-}C_6H_6)(\mu_3\text{-}\eta^2\text{:}\eta^2\text{:}\eta^2\text{-}C_6H_6)]$. Analogously, the CO-ligand distribution recalls that observed in this latter compound, in $[Ru_6C(CO)_{17}]$, and most of the known substituted derivatives, *i.e.* with one CO occupying a bridging position along one edge of the molecular equator, while the remaining ten CO ligands show different degrees of symmetry and bending in the two crystal lattices.

Table 2 NOE data (% enhancement) for compounds **2a**–**2d**

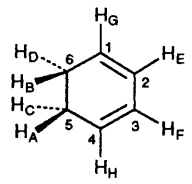

	Irradiation site							
	A	B	C	D	E	F	G	H
A			19					
B				17				
C	17							6
D		16					6	
E						8	6	
F					7			6
G		2		6	7			
H	2		6			7		

Table 3 Proton NMR data for compounds **2a**–**2d** and **3a**–**3d**

	δ(^{1}H)		
Compound	Arene	Me	
2a	5.51 (6 H)		
2b	5.59 (t of d, 1 H), 5.53 (t of d, 1 H), 5.49 (d, 1 H), 5.47 (d, 1 H), 5.21 (t of t, 1 H)	2.22 (3 H)	
2c	5.59 (m, 2 H), 5.23 (m, 2 H)	2.26 (3 H), 2.23 (3 H)	
2d	5.33 (3 H)	2.30 (6 H)	
	$\mu_3\text{-}\eta^2\text{:}\eta^2\text{:}\eta^2\text{-}C_6H_6$	η^6-arene	Me
3a	4.14 (6 H)	5.54 (6 H)	
3b	4.12 (6 H)		
3c	4.10 (6 H)	5.53 (m, 2 H), 5.27 (m, 2 H)	2.26 (6 H)
3d	4.09 (6 H)	5.55 (3 H)	2.29 (9 H)

As mentioned above, there are two independent molecules in the asymmetric unit of **3c**. Fig. 4 shows a comparative projection of the two molecules of **3c** (A and B) as well as that of **3b**. Taking the bridging CO as reference, it can be appreciated that the three molecules differ slightly (but significantly) in the rotameric conformation of the toluene and of the two xylene ligands. Conformational freedom of the apical ligands had been previously seen in the case of the two crystalline forms of $[Ru_6C(CO)_{17}]$,[19] and for the mono(arene) derivatives $[Ru_6C(CO)_{14}(\eta^6\text{-arene})]$ **2a**, **2b** and **2d**. As in all these cases, the difference between molecules **A** and **B** can be ascribed to the optimisation of intermolecular packing interactions in the presence of a shallow conformational potential. Molecule **3b** possesses molecular and crystallographic *m* symmetry with the mirror plane bisecting both arene ligands and comprising of the unique bridging CO, the methyl group and the C(carbide) atom.

A comparison of some relevant structural parameters is also noteworthy, those related to **3c** will be given as pairs of chemically equivalent values over the two independent structures. The Ru–Ru bond lengths range from 2.798(1) to 2.950(1) Å in **3b**, and from 2.819(1) to 3.015(1) Å and 2.805(1) to 2.980(1) Å in molecules A and B of **3c** respectively. Interestingly, only in **3b** the shortest bond length is the one spanned by the bridging CO ligand, while in both molecules of **3c** the shortest bonds involve an unbridged edge and one arene-bridged edge, respectively. Analogously, the longest bond in **3b** is an

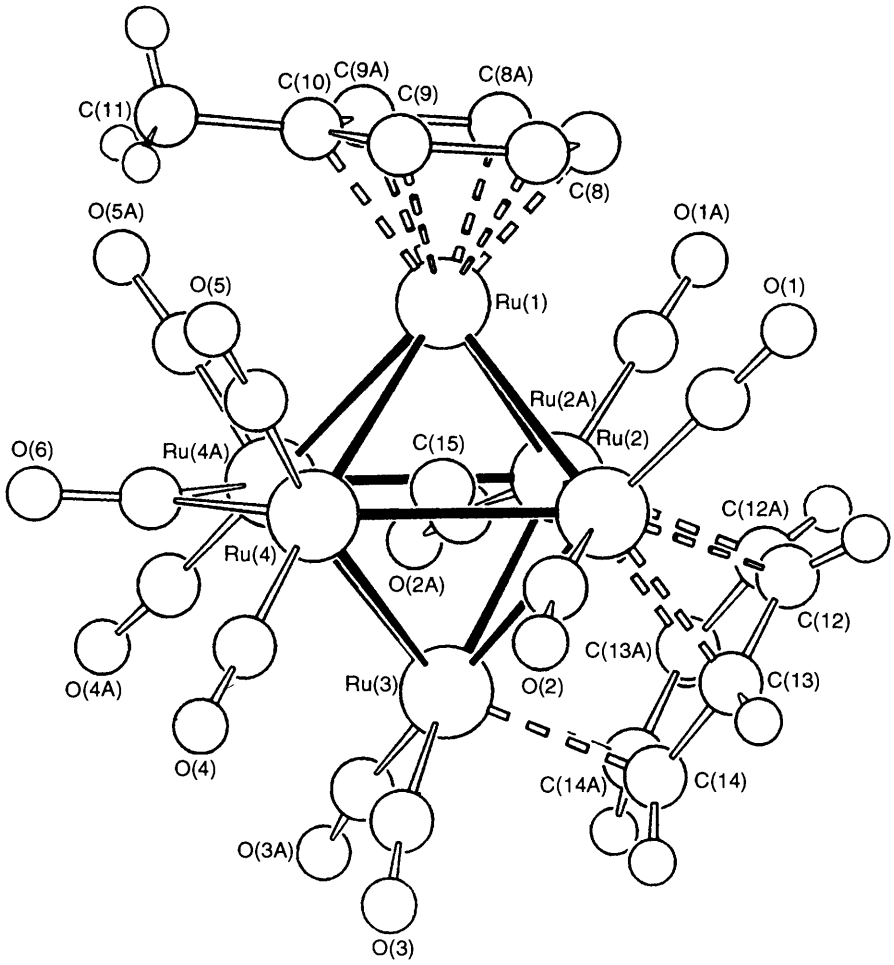

Fig. 2 The molecular structure of compound **3b** in the solid state. The C atoms of the CO groups bear the same labelling as the corresponding O atoms

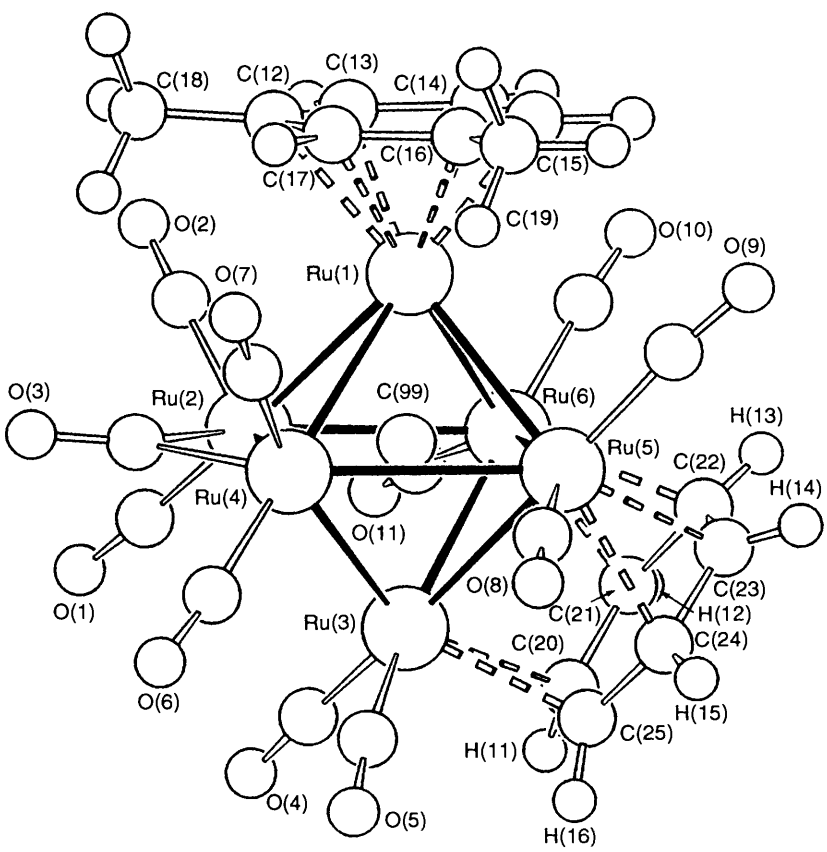

Fig. 3 The molecular structure of compound **3c** in the solid state. Note that only one (molecule A) of the two independent molecules is shown. The C atoms of the CO groups bear the same labelling as the corresponding O atoms

equatorial, arene-bridged, edge [Ru(2)–Ru(2A)], while in both molecules A and B of **3c** it is the one joining the CO-bridged equatorial edge [Ru(6)–Ru(5) in Ru(2a)–Ru(5a) in B]. These differences, coupled with the large and statistically significant differences in bond length ranges (chemically equivalent bonds show differences that are one order of magnitude larger than the e.s.d.s on the individual values) confirm our previous observations that the metal cores in transition-metal clusters are highly deformable and capable of 'adapting' the molecule to the steric requirements of the surroundings with very small expenditure of internal bonding energy.[20]

The Ru–C(carbide) distances in both **3b** and **3c** show the expected 'drift' of the interstitial atom towards the Ru atom bearing the η^6-bound arene. This effect is present systematically in all arene-substituted clusters. Bond lengths Ru(1)–C(15) in **3b**, Ru(1)–C(99) (**3c** molecule A) and Ru(1A)–C(99A) (**3c**, molecule B) are 1.94(1), 1.93(1) and 1.91(1) Å, respectively, while the remaining Ru–C(carbide) bond distances average 2.04(1) Å in the three compounds.

It is interesting that the out-of-plane bending of the H atoms bound to the face-capping benzene ligands observed in $[Ru_3(CO)_9(\mu_3\text{-}\eta^2:\eta^2:\eta^2\text{-}C_6H_6)]$[14] is also clearly visible in **3b** and **3c** (see Experimental section for a description of how the H-atom modelling was done in molecule **3c**).

The crystal structures of **3b** and **3c** have also been investigated. Empirical calculations within the atom–atom pairwise packing potential energy method and computer graphics have proved to be a useful tool for studying the molecular organisation in the lattice of the transition-metal cluster molecules and ions, and have now been applied here.[21]

By this means we have previously shown that arene clusters tend to establish very interesting packing structures in their lattice. For instance, in the case of crystalline $[Ru_6C(CO)_{11}(\eta^6\text{-}C_6H_6)(\mu_3\text{-}\eta^2:\eta^2:\eta^2\text{-}C_6H_6)]$, we found that the two benzene ligands 'link' together molecules in the lattice *via* benzene–benzene graphitic-like interactions.[22] This preferential pattern of intermolecular linkage has also been observed in related molecules such as $[Ru_6C(CO)_{11}(\eta^6\text{-}C_6H_3Me_3\text{-}1,3,5)(\eta^6\text{-}C_6H_6)]$ and $[Ru_6C(CO)_{11}(\eta^6\text{-}C_6H_3Me_3\text{-}1,3,5)_2]$.[16]

The molecular organisation in crystalline **3b** closely resembles that observed in crystals of the bis(arene) complexes mentioned above: molecular 'snakes' are formed as shown in Fig. 5. The toluene and benzene fragments belonging to next neighbouring molecules face each other in the chain, although the presence of the methyl group on the toluene fragment prevents the two arenes from being parallel as, for example, in $[Ru_6C(CO)_{11}(\eta^6\text{-}C_6H_6)(\mu_3\text{-}\eta^2:\eta^2:\eta^2\text{-}C_6H_6)]$. In crystalline **3c** the packing is more complicated being basically formed by 'dimers' of benzene–benzene interaction molecules. Fig. 6 shows a simplifed space-filling projection of the molecular organisation in this lattice. Note how the CH_2Cl_2 molecules are wedged in between the two benzene fragments, while the xylene

Table 4 Selected bond lengths (Å) and angles (°) for compound **3b**

Ru(1)–Ru(2)	2.870(1)	Ru(1)–C(15)	1.942(8)
Ru(1)–Ru(4)	2.891(1)	Ru(2)–C(15)	2.033(5)
Ru(2)–Ru(2A)	2.950(1)	Ru(3)–C(15)	2.062(8)
Ru(2)–Ru(3)	2.817(1)	Ru(4)–C(15)	2.085(5)
Ru(2)–Ru(4)	2.942(1)		
Ru(3)–Ru(4)	2.908(1)	Ru(4)–C(6)	2.035(6)
Ru(4)–Ru(4A)	2.798(1)		
Ru(1)–C(8)	2.225(6)	Ru(2)–C(12)	2.283(6)
Ru(1)–C(9)	2.249(6)	Ru(2)–C(13)	2.208(6)
Ru(1)–C(10)	2.265(9)	Ru(3)–C(14)	2.288(6)
C(7)–C(8)	1.416(8)	C(12)–C(12A)	1.45(1)
C(8)–C(9)	1.401(9)	C(12)–C(13)	1.398(9)
C(9)–C(10)	1.405(7)	C(13)–C(14)	1.417(9)
C(10)–C(11)	1.51(1)	C(14)–C(14A)	1.43(1)
C(8A)–C(7)–C(8)	119.6(1.0)	C(12)–C(13)–C(14)	119.1(5)
C(7)–C(8)–C(9)	119.6(6)	Ru(2)–C(2)–O(2)	172.1(5)
C(8)–C(9)–C(10)	121.2(6)	Ru(4A)–C(6)–Ru(4)	86.9(3)
C(9)–C(10)–C(9A)	118.1(9)		

Table 5 Selected bond lengths (Å) and angles (°) for **3c**

Molecule A		Molecule B		Molecule A		Molecule B	
Ru(1)–Ru(2)	2.883(1)	Ru(1A)–Ru(2A)	2.876(1)	Ru(1)–C(15)	2.239(13)	Ru(1A)–C(15A)	2.211(13)
Ru(1)–Ru(4)	2.884(1)	Ru(1A)–Ru(4A)	2.917(1)	Ru(1)–C(16)	2.266(13)	Ru(1A)–C(16A)	2.267(15)
Ru(1)–Ru(5)	2.865(1)	Ru(1A)–Ru(5A)	2.874(1)	Ru(1)–C(17)	2.264(12)	Ru(1A)–C(17A)	2.253(13)
Ru(1)–Ru(6)	2.911(1)	Ru(1A)–Ru(6A)	2.856(1)	C(12)–C(13)	1.392(19)	C(12A)–C(13A)	1.403(21)
Ru(2)–Ru(3)	2.908(1)	Ru(2A)–Ru(3A)	2.919(1)	C(13)–C(14)	1.432(18)	C(13A)–C(14A)	1.401(24)
Ru(2)–Ru(4)	2.827(1)	Ru(2A)–Ru(4A)	2.805(1)	C(14)–C(15)	1.420(18)	C(14A)–C(15A)	1.470(29)
Ru(2)–Ru(6)	2.869(1)	Ru(2A)–Ru(6A)	2.980(1)	C(15)–C(16)	1.420(19)	C(15A)–C(16A)	1.406(25)
Ru(3)–Ru(4)	2.872(1)	Ru(3A)–Ru(4A)	2.915(1)	C(16)–C(17)	1.399(19)	C(16A)–C(17A)	1.425(19)
Ru(3)–Ru(5)	2.819(1)	Ru(3A)–Ru(5A)	2.820(1)	C(17)–C(12)	1.443(17)	C(17A)–C(12A)	1.372(24)
Ru(3)–Ru(6)	2.824(1)	Ru(3A)–Ru(6A)	2.915(1)	C(12)–C(18)	1.499(22)	C(12A)–C(18A)	1.499(22)
Ru(4)–Ru(5)	3.015(1)	Ru(4A)–Ru(5A)	2.865(1)	C(16)–C(19)	1.469(19)	C(16A)–C(19A)	1.549(22)
Ru(5)–Ru(6)	2.908(1)	Ru(5A)–Ru(6A)	2.954(1)	Ru(3)–C(20)	2.309(7)	Ru(3A)–C(20A)	2.191(9)
Ru(1)–C(99)	1.925(9)	Ru(1A)–C(99A)	1.907(11)	Ru(3)–C(25)	2.220(7)	Ru(3A)–C(25A)	2.352(10)
Ru(2)–C(99)	2.081(8)	Ru(2A)–C(99A)	2.068(10)	Ru(5)–C(23)	2.243(7)	Ru(5A)–C(23A)	2.297(9)
Ru(3)–C(99)	2.083(9)	Ru(3A)–C(99A)	2.108(11)	Ru(5)–C(24)	2.283(8)	Ru(5A)–C(24A)	2.201(10)
Ru(4)–C(99)	2.049(9)	Ru(4A)–C(99A)	2.044(10)	Ru(6)–C(21)	2.210(8)	Ru(6A)–C(21A)	2.276(10)
Ru(5)–C(99)	2.028(8)	Ru(5A)–C(99A)	2.041(10)	Ru(6)–C(22)	2.344(7)	Ru(6A)–C(22A)	2.262(10)
Ru(6)–C(99)	2.073(8)	Ru(6A)–C(99A)	2.068(10)	C(20)–C(21)	1.432(10)	C(20A)–C(21A)	1.446(14)
C(3)–Ru(2)	2.051(12)	C(3A)–Ru(2A)	2.045(14)	C(21)–C(22)	1.469(10)	C(21A)–C(22A)	1.472(13)
C(3)–Ru(4)	2.056(12)	C(3A)–Ru(4A)	2.067(16)	C(22)–C(23)	1.420(10)	C(22A)–C(23A)	1.391(12)
Ru(1)–C(12)	2.281(14)	Ru(1A)–C(12A)	2.224(13)	C(23)–C(24)	1.385(10)	C(23A)–C(24A)	1.455(14)
Ru(1)–C(13)	2.227(13)	Ru(1A)–C(13A)	2.238(16)	C(24)–C(25)	1.455(10)	C(24A)–C(25A)	1.384(13)
Ru(1)–C(14)	2.226(12)	Ru(1A)–C(14A)	2.246(20)	C(25)–C(20)	1.388(10)	C(25A)–C(20A)	1.436(12)
C(12)–C(13)–C(14)	120(1)	C(12A)–C(13A)–C(14A)	118(1)	C(22)–C(23)–C(24)	124(1)	C(22A)–C(23A)–C(24A)	124(1)
C(13)–C(14)–C(15)	120(1)	C(13A)–C(14A)–C(15A)	121(1)	C(23)–C(24)–C(25)	117(1)	C(23A)–C(24A)–C(25A)	118(1)
C(14)–C(15)–C(16)	121(1)	C(14A)–C(15A)–C(16A)	118(1)	C(24)–C(25)–C(26)	121(1)	C(24A)–C(25A)–C(20A)	124(1)
C(15)–C(16)–C(17)	118(1)	C(15A)–C(16A)–C(17A)	119(1)	C(25)–C(20)–C(27)	122(1)	C(25A)–C(20A)–C(21A)	118(1)
C(16)–C(17)–C(12)	123(1)	C(16A)–C(17A)–C(12A)	121(1)	Ru(2)–C(3)–Ru(4)	87(1)	Ru(2A)–C(3A)–Ru(4A)	85(1)
C(17)–C(12)–C(13)	119(1)	C(17A)–C(12A)–C(13A)	122(1)	Ru(5)–C(8)–O(8)	175(1)	Ru(5A)–C(8A)–O(8A)	171(1)
C(20)–C(21)–C(22)	118(1)	C(20A)–C(21A)–C(22A)	120(1)	Ru(6)–C(11)–O(11)	171(1)	Ru(6A)–C(11A)–O(11A)	177(1)
C(21)–C(22)–C(23)	117(1)	C(21A)–C(22A)–C(23A)	118(1)				

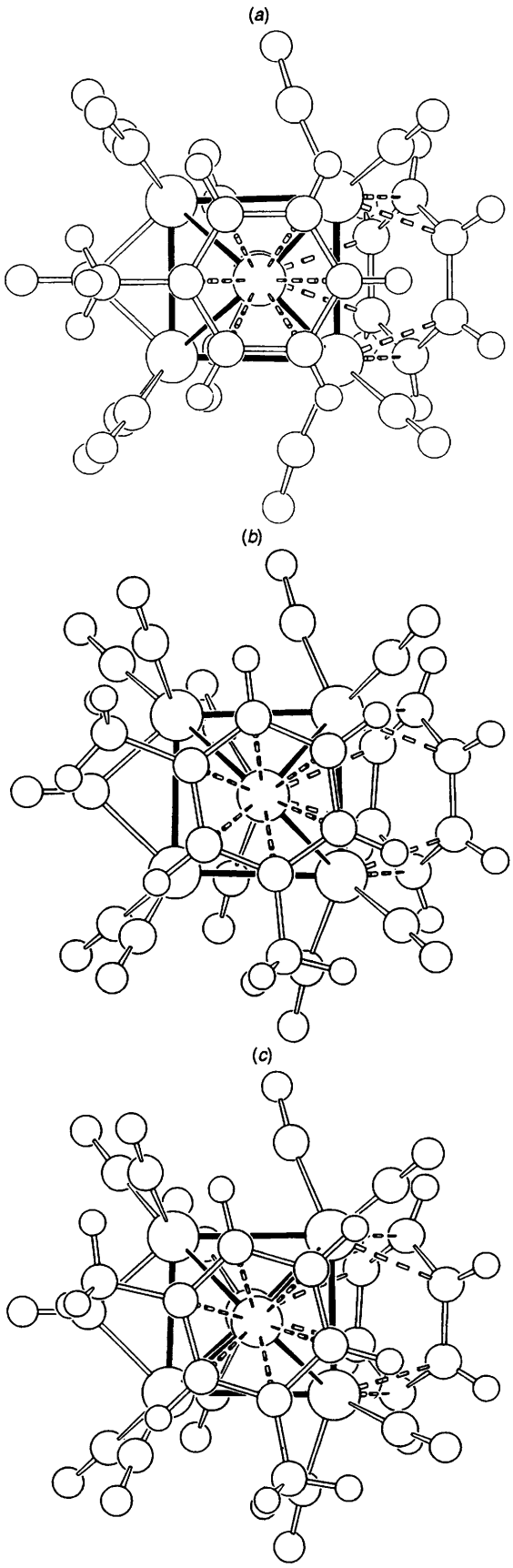

Fig. 4 Comparative projection of **3b** (*a*) and the two independent molecules of **3c** (*b*) and (*c*) showing the different rotameric conformation of the η^6-arene ligands with respect to the CO-bridged octahedron equator

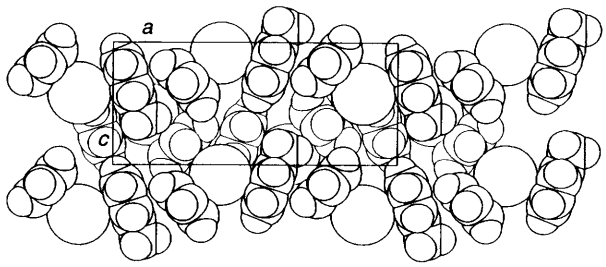

Fig. 5 Molecular organisation in crystalline **3b** showing how the benzene and toluene ligands belonging to neighbouring molecules are almost face to face forming a 'snake' throughout the crystal. For clarity, the CO ligands are omitted and the cluster core is represented by a large sphere

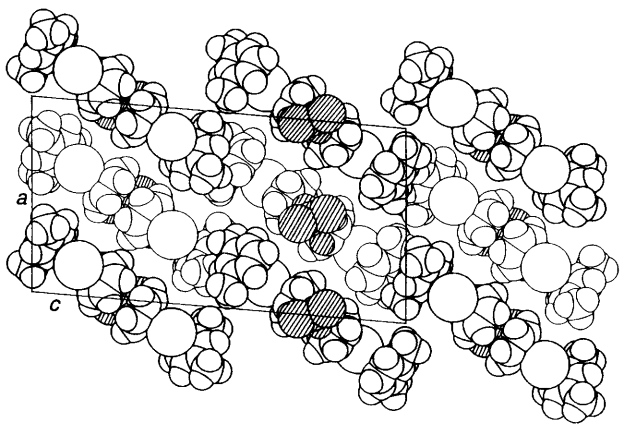

Fig. 6 Molecular organisation in crystalline **3c** showing how the two independent molecules present in the unit cell are bridged by the CH_2Cl_2 solvent molecules. Other details as in Fig. 5

ligands tend to form ribbons throughout the crystal lattice. Similar packing patterns had been previously observed in the crystal of some mono(arene) clusters such as $[Os_4H_2(CO)_{10}(\eta^6\text{-arene})]$ (arene = C_6H_6 or C_6H_5Me) and $[Ru_6C(CO)_{14}(\eta^6\text{-}C_6H_5Me)]$.[23] It is, however, difficult, to say whether the crystallisation of **3c** with two independent molecules *and* one solvent molecule is due to a kinetic control over the crystallisation process or if this reflects a true difficulty in packing molecules carrying the 'asymmetric' xylene ligand. It is interesting, in this context, that the analogous xylene cluster $[Os_4H_2(CO)_{10}(\eta^6\text{-}C_6H_4Me_2\text{-}1,3)]$, besides being affected by orientational disorder of the arene fragments, also crystallises with two independent molecules in the asymmetric unit.

We are currently investigating the other bis(arene) derivatives of the hexaruthenium–carbido cluster system, which shall be reported in due course. A detailed analysis of all these arene cluster species regarding the molecular organisation and crystal packing will be the subject of a future report.

Experimental

All reactions were carried out with the exclusion of air using solvents freshly distilled under an atmosphere of nitrogen. Subsequent work-up of products was achieved without precautions to exclude air. Infrared spectra were recorded on a Perkin Elmer 1600 Series Fourier-transform spectrometer in CH_2Cl_2 using NaCl cells. Positive fast atom bombardment mass spectra were obtained using a Kratos MS50TC spectrometer, using CsI as calibrant. Proton NMR spectra were recorded in $CDCl_3$ using a Bruker AM360 instrument, and referenced to internal $SiMe_4$. The COSY experiments were recorded over a range of 230 Hz in F2 (1150 Hz in F1) using a magnitude mode experiment. A relaxation delay of 3 s was used.

Table 6 Crystal data and details of measurements for compounds **3b** and **3c**

	3b	**3c**
Formula	$C_{25}H_{14}O_{11}Ru_6$	$C_{26}H_{16}O_{11}Ru_6 \cdot CH_2Cl_2$
M	1096.79	1195.76
Crystal system	Orthorhombic	Monoclinic
Crystal dimensions/mm	0.10 × 0.08 × 0.10	0.07 × 0.08 × 0.11
Space group	*Pnma*	$P2_1/n$
a/Å	9.035(5)	18.27(2)
b/Å	14.796(2)	9.729(2)
c/Å	20.534(4)	34.39(2)
β/°	—	94.94(6)
U/Å^3	2745	6090
Z	4	8
F(000)	2063	4360
λ(Mo-Kα)/Å	0.710 69	0.710 69
μ(Mo-Kα)/cm^{-1}	29.80	27.71
θ range/°	2.5–25	2.5–25
ω-scan width/°	0.90	0.80
Requested counting σ(I)/I	0.02	0.02
Prescan rate/° min^{-1}	5	8
Prescan acceptance σ(I)/I	0.5	0.5
Maximum scan time/s	90	60
Octants explored	$\pm h, \pm k, +l$[a]	$\pm h, +k, +l$
Measured reflections	9434	11 578
Unique observed reflections [$I_o > 2\sigma(I_o)$]	1770	7833
No. of refined parameters	226	785
R,R',[b] S	0.020—,[c] 2.6	0.058, 0.062, 4.6
k, g[b]	1, —[c]	4.15, 0.000 74

[a] Intensity data for **3b** were collected in the triclinic system, but the structure was solved in the orthorhombic system. [b] $R' = \Sigma[(F_o - F_c)w^{\frac{1}{2}}]/\Sigma F_o w^{\frac{1}{2}}$, where $w = k/[\sigma(F) + |g|F^2]$. [c] Unit weights were used in the refinement of **3b**.

Table 7 Fractional atomic coordinates for compound **3b**

Atom	x	y	z
Ru(1)	0.027 10(3)	0.250 00	0.638 54(7)
Ru(2)	0.139 47(2)	0.150 31(3)	0.733 58(4)
Ru(3)	0.216 60(3)	0.250 00	0.534 04(7)
Ru(4)	0.103 34(2)	0.155 44(3)	0.418 61(4)
C(15)	0.118 8(4)	0.250 0	0.586 1(8)
C(1)	0.091 0(3)	0.088 7(4)	0.881 0(6)
O(1)	0.062 5(2)	0.050 5(3)	0.969 3(5)
C(2)	0.157 3(3)	0.039 9(4)	0.639 3(6)
O(2)	0.172 7(2)	−0.029 4(3)	0.595 5(5)
C(3)	0.262 8(3)	0.159 6(5)	0.432 5(7)
O(3)	0.294 8(3)	0.103 0(5)	0.383 2(7)
C(4)	0.148 9(3)	0.078 8(4)	0.290 3(6)
O(4)	0.174 2(2)	0.029 7(3)	0.211 0(5)
C(5)	0.030 3(3)	0.088 4(4)	0.374 3(6)
O(5)	−0.014 3(2)	0.046 3(3)	0.337 8(5)
C(6)	0.083 6(4)	0.250 0	0.261 4(9)
O(6)	0.066 3(3)	0.250 0	0.137 0(6)
C(7)	−0.032 1(4)	0.250 0	0.841 5(10)
C(8)	−0.043 5(3)	0.167 3(4)	0.767 1(7)
C(9)	−0.064 9(3)	0.168 3(4)	0.619 8(7)
C(10)	−0.075 1(4)	0.250 0	0.544 1(10)
C(11)	−0.100 8(6)	0.250 0	0.387 8(12)
C(12)	0.200 2(3)	0.200 9(4)	0.928 3(6)
C(13)	0.238 7(3)	0.153 1(4)	0.827 7(7)
C(14)	0.279 0(3)	0.201 6(4)	0.728 3(7)

Products were separated by thin layer chromatography (TLC) on plates supplied by Merck coated with a 0.25 mm layer of Kieselgel 60 F_{254} using hexane–dichloromethane (7:3) as eluent. $[Ru_5C(CO)_{15}]$ and $[Ru(arene)(MeCN)_3]^{2+}$ (arene = C_6H_6, C_6H_5Me, $C_6H_4Me_2$-1,3 or $C_6H_3Me_3$-1,3,5) were prepared by literature procedures.[23,24] Cyclohexa-1,3-diene and cyclohexa-1,4-diene were purchased from Aldrich and used without further purification. Trimethylamine *N*-oxide (Me_3NO) was sublimed prior to reaction.

Preparation of $[Ru_6C(CO)_{14}(\eta^6\text{-arene})]$ (*arene* = C_6H_6 **1a**, C_6H_5Me **1b**, $C_6H_4Me_2$-1,3 **1c** *or* $C_6H_3Me_3$-1,3,5 **1d**).—In a typical reaction $[N(PPh_3)_2][Ru_5C(CO)_{14}]$ (200 mg) in CH_2Cl_2 (30 cm^3) was added dropwise to a refluxing solution of $[Ru(arene)(MeCN)_3][BF_4]_2$ (1.1 mol equivalent) in CH_2Cl_2 (30 cm^3). A total reflux time of 20 min was adequate to ensure complete reaction of the starting material. The resulting brown solution was filtered through a short column containing silica gel (60 mesh, 2 cm), the solvent removed *in vacuo* and the product characterised as $[Ru_6C(CO)_{14}(\eta^6\text{-arene})]$ (80–90%).

Preparation of $[Ru_6C(CO)_{12}(\eta^6\text{-arene})(\mu\text{-}\eta^2\text{:}\eta^2\text{-}C_6H_8)]$ (*arene* = C_6H_6 **2a**, C_6H_5Me **2b**, $C_6H_4Me_2$-1,3 **2c** or $C_6H_3Me_3$-1,3,5 **2d**) *and* $[Ru_6C(CO)_{11}(\eta^6\text{-arene})(\mu_3\text{-}\eta^2\text{:}\eta^2\text{:}\eta^2\text{-}C_6H_6)]$ (*arene* = C_6H_6 **3a**, C_6H_5Me **3b**, $C_6H_4Me_2$-1,3 **3c** *or* $C_6H_3Me_3$-1,3,5 **3d**).—Typically, $[Ru_6C(CO)_{14}(\eta^6\text{-arene})]$ (30 mg) in CH_2Cl_2 (30 cm^3) containing an excess of cyclohexa-1,3-diene or cyclohexa-1,4-diene (1.5 cm^3) was treated with Me_3NO (2.2 mol equivalents) added dropwise in CH_2Cl_2 (5 cm^3). The reaction mixture was stirred for 25 min, after which time the solvent was removed *in vacuo* and the products separated by TLC. The major brown band was $[Ru_6C(CO)_{12}(\eta^6\text{-arene})(\mu\text{-}\eta^2\text{:}\eta^2\text{-}C_6H_8)]$ (20–30%), the minor red band $[Ru_6C(CO)_{11}(\eta^6\text{-arene})(\mu_3\text{-}\eta^2\text{:}\ \eta^2\text{:}\eta^2\text{-}C_6H_6)]$ (5–10%) (Found: C, 27.30; H, 1.20. $C_{25}H_{14}O_{11}Ru_6$ **3b** requires C, 27.35; H, 1.30. Found: C, 27.95; H, 1.50. $C_{26}H_{16}O_{11}Ru_6$ **3c** requires C, 28.10; H, 1.45%).

Conversion of $[Ru_6C(CO)_{12}(\eta^6\text{-arene})(\mu\text{-}\eta^2\text{:}\eta^2\text{-}C_6H_8)]$ **2a–2d** *to* $[Ru_6C(CO)_{11}(\eta^6\text{-arene})(\mu_3\text{-}\eta^2\text{:}\eta^2\text{:}\eta^2\text{-}C_6H_6)]$ **3a–3d**.—In a typical reaction, $[Ru_6C(CO)_{12}(\eta^6\text{-arene})(\mu\text{-}\eta^2\text{:}\eta^2\text{-}C_6H_8)]$ (10 mg) in CH_2Cl_2 (20 cm^3) was cooled to −78 °C and treated with Me_3NO (1.1 mol equivalents) added dropwise in CH_2Cl_2 (5 cm^3). The solution was allowed to warm to room temperature, the solvent removed *in vacuo*, and the products separated by TLC. The two bands consist of the brown starting material, $[Ru_6C(CO)_{12}(\eta^6\text{-arene})(\mu\text{-}\eta^2\text{:}\eta^2\text{-}C_6H_8)]$, and $[Ru_6C(CO)_{11}(\eta^6\text{-arene})(\mu_3\text{-}\eta^2\text{:}\eta^2\text{:}\eta^2\text{-}C_6H_6)]$ (5–10%).

Interconversion of $[Ru_6C(CO)_{11}(\eta^6\text{-arene})(\mu_3\text{-}\eta^2\text{:}\eta^2\text{:}\eta^2\text{-}C_6H_6)]$ **3a–3d** *and* $[Ru_6C(CO)_{11}(\eta^6\text{-arene})(\eta^6\text{-}C_6H_6)]$ **4a–4d**.—Typically, $[Ru_6C(CO)_{11}(\eta^6\text{-arene})(\mu_3\text{-}\eta^2\text{:}\eta^2\text{:}\eta^2\text{-}C_6H_6)]$ (5 mg) in CH_2Cl_2 (10 cm^3) was stored at −25 °C, and monitored periodically by IR spectroscopy. Over a period of 10–15 weeks, isomerisation to $[Ru_6C(CO)_{11}(\eta^6\text{-arene})(\eta^6\text{-}C_6H_6)]$ had occurred (30–95%).

Upon refluxing $[Ru_6C(CO)_{11}(\eta^6\text{-arene})(\eta^6\text{-}C_6H_6)]$ (2 mg) in hexane (20 cm^3) for 7 h the regeneration of $[Ru_6C(CO)_{11}(\eta^6\text{-arene})(\mu_3\text{-}\eta^2\text{:}\eta^2\text{:}\eta^2\text{-}C_6H_6)]$ (30–50%) was observed as monitored by IR spectroscopy.

Structural Characterisation of **3b** *and* **3c**.—The diffraction data for both **3b** and **3c** were collected on an Enraf–Nonius CAD-4 diffractometer equipped with a graphite monochromator (Mo-Kα radiation, λ = 0.710 69 Å). Crystal data and details of measurements are summarised in Table 6. The structures were solved by direct methods, which allowed for the location of the ruthenium atoms, followed by Fourier difference syntheses and subsequent least-squares refinement.[25] For all calculations the SHELX 76 program was used.[26] All atoms were refined anisotropically in both structures with the exception of the hydrogen atoms which were attributed common isotropic thermal parameters. The hydrogen atoms of the benzene ligand in **3b** and in molecule A of **3c** were located directly from final Fourier difference syntheses and refined with constraints on the C–H distances. The modelling of the hydrogen atoms posed some problem in the structure of molecule B of **3c**. The non-

Table 8 Fractional atomic coordinates for compound **3c**

Atom	*x*	*y*	*z*	Atom	*x*	*y*	*z*
Ru(1)	0.693 97(4)	0.564 09(8)	0.095 71(2)	Ru(1A)	0.293 94(5)	0.548 92(10)	0.415 96(3)
Ru(2)	0.738 38(4)	0.299 01(8)	0.126 91(2)	Ru(2A)	0.402 57(5)	0.336 62(10)	0.411 86(3)
Ru(3)	0.598 65(4)	0.287 33(8)	0.161 40(2)	Ru(3A)	0.410 16(5)	0.411 40(11)	0.330 10(3)
Ru(4)	0.605 42(4)	0.322 42(8)	0.078 87(2)	Ru(4A)	0.274 40(5)	0.321 15(10)	0.360 91(3)
Ru(5)	0.558 01(4)	0.548 36(8)	0.131 20(3)	Ru(5A)	0.291 86(5)	0.596 08(10)	0.333 36(3)
Ru(6)	0.695 65(4)	0.509 03(8)	0.178 98(2)	Ru(6A)	0.428 79(5)	0.622 44(10)	0.385 15(3)
C(99)	0.648 2(4)	0.429 7(9)	0.126 8(3)	C(99A)	0.346 9(5)	0.476 9(10)	0.375 1(3)
C(1)	0.776 8(7)	0.134 5(15)	0.148 2(4)	C(1A)	0.473 2(7)	0.199 2(15)	0.411 3(5)
O(1)	0.803 4(7)	0.035 6(11)	0.161 1(3)	O(1A)	0.515 3(6)	0.112 7(13)	0.412 1(5)
C(2)	0.833 7(7)	0.334 0(13)	0.116 2(4)	C(2A)	0.413 7(7)	0.325 8(16)	0.465 8(5)
O(2)	0.893 8(5)	0.355 5(13)	0.112 5(4)	O(2A)	0.423 4(7)	0.313 4(14)	0.498 9(3)
C(3)	0.698 6(7)	0.205 7(12)	0.075 9(4)	C(3A)	0.315 8(7)	0.198 4(15)	0.406 7(5)
O(3)	0.718 7(6)	0.124 8(11)	0.053 8(3)	O(3A)	0.301 8(6)	0.097 8(12)	0.421 4(4)
C(4)	0.641 1(7)	0.130 5(14)	0.187 0(4)	C(4A)	0.504 4(8)	0.327 1(15)	0.338 4(4)
O(4)	0.665 0(6)	0.033 9(11)	0.202 7(4)	O(4A)	0.562 9(5)	0.288 6(15)	0.342 5(4)
C(5)	0.515 5(6)	0.183 9(12)	0.141 4(3)	C(5A)	0.382 8(8)	0.287 5(17)	0.289 1(5)
O(5)	0.464 5(5)	0.123 8(11)	0.133 7(3)	O(5A)	0.366 5(8)	0.223 6(15)	0.262 2(4)
C(6)	0.542 3(7)	0.173 7(14)	0.062 5(4)	C(6A)	0.260 3(8)	0.170 0(17)	0.327 0(5)
O(6)	0.506 7(6)	0.084 6(11)	0.050 0(3)	O(6A)	0.247 2(8)	0.079 6(13)	0.307 0(4)
C(7)	0.593 2(6)	0.379 2(13)	0.027 6(3)	C(7A)	0.174 9(7)	0.310 0(16)	0.368 6(4)
O(7)	0.578 9(6)	0.414 1(12)	−0.004 3(3)	O(7A)	0.114 3(6)	0.295 6(14)	0.368 8(4)
C(8)	0.473 1(6)	0.495 7(15)	0.100 4(4)	C(8A)	0.233 8(8)	0.492 1(15)	0.297 0(4)
O(8)	0.418 6(5)	0.465 5(13)	0.084 2(3)	O(8A)	0.199 7(7)	0.439 2(12)	0.270 5(3)
C(9)	0.548 1(6)	0.737 3(15)	0.118 0(4)	C(9A)	0.215 9(8)	0.727 3(15)	0.335 4(4)
O(9)	0.540 5(7)	0.851 5(11)	0.113 5(4)	O(9A)	0.167 3(5)	0.804 9(11)	0.336 2(3)
C(10)	0.756 7(7)	0.664 4(12)	0.191 3(3)	C(10A)	0.517 8(7)	0.552 0(14)	0.407 4(4)
O(10)	0.791 6(5)	0.752 8(10)	0.200 6(3)	O(10A)	0.577 9(5)	0.518 9(13)	0.417 3(3)
C(11)	0.768 2(6)	0.393 4(13)	0.204 3(3)	C(11A)	0.439 1(7)	0.776 6(15)	0.419 5(5)
O(11)	0.808 1(5)	0.331 8(11)	0.223 8(3)	O(11A)	0.447 1(8)	0.865 6(12)	0.441 0(4)
C(12)	0.777 0(7)	0.569 0(13)	0.049 8(4)	C(12A)	0.309 7(7)	0.638 0(17)	0.475 7(4)
C(13)	0.806 7(7)	0.630 6(14)	0.084 2(4)	C(13A)	0.281 5(10)	0.741 7(16)	0.450 3(4)
C(14)	0.769 5(7)	0.744 0(12)	0.100 3(4)	C(14A)	0.214 6(10)	0.716 5(21)	0.428 3(5)
C(15)	0.700 5(7)	0.789 0(13)	0.082 6(4)	C(15A)	0.178 8(7)	0.581 3(23)	0.429 0(4)
C(16)	0.667 8(6)	0.723 6(14)	0.048 5(4)	C(16A)	0.208 2(7)	0.483 3(21)	0.456 1(4)
C(17)	0.706 7(7)	0.616 7(14)	0.032 5(3)	C(17A)	0.274 8(7)	0.514 3(20)	0.479 1(4)
C(18)	0.815 9(9)	0.459 5(18)	0.028 9(5)	C(18A)	0.377 1(10)	0.666 0(18)	0.502 5(4)
C(19)	0.599 0(8)	0.769 1(20)	0.027 2(6)	C(19A)	0.169 4(11)	0.324 9(29)	0.459 9(5)
C(20)	0.587 8(4)	0.370 6(7)	0.223 5(2)	C(20A)	0.474 0(5)	0.571 3(9)	0.303 5(3)
C(21)	0.631 2(4)	0.492 2(7)	0.230 3(2)	C(21A)	0.488 3(5)	0.679 6(9)	0.332 0(3)
C(22)	0.604 7(4)	0.620 4(7)	0.211 3(2)	C(22A)	0.430 9(5)	0.782 2(9)	0.337 5(3)
C(23)	0.533 8(4)	0.618 6(7)	0.190 9(2)	C(23A)	0.364 7(5)	0.772 2(9)	0.314 5(3)
C(24)	0.492 8(4)	0.500 4(7)	0.183 3(2)	C(24A)	0.350 0(5)	0.670 0(9)	0.284 0(3)
C(25)	0.520 8(4)	0.373 3(7)	0.201 2(2)	C(25A)	0.405 4(5)	0.575 6(9)	0.279 7(3)
C(1S)	0.502 3(15)	0.082 6(24)	0.742 8(6)	Cl(2)	0.460 0(4)	−0.040 0(7)	0.711 7(2)
Cl(1)	0.524 1(4)	0.023 3(6)	0.788 5(2)				

coplanarity of the C and H atoms prevented direct use of the usual D_{6h} model. In order to obtain a more reliable model, the hydrogen atoms in this molecule were placed at the same average out-of-plane bending angle observed in molecule A and then refined together with the C_6 moiety as a rigid body. Fractional atomic coordinates for **3b** and **3c** are listed in Tables 7 and 8, respectively.

Additional material available from the Cambridge Crystallographic Data Centre comprises H-atom coordinates, thermal parameters and remaining bond lengths and angles.

Acknowledgements

We would like to thank the SERC and British Petroleum (P. L. D.) for financial assistance. Financial support (Italy) is also acknowledged (to D. B., F. G.). D. B., F. G. and B. F. G. J. acknowledge NATO for a travel grant.

References

1 B. F. G. Johnson, R. D. Johnston and J. Lewis, *Chem. Commun.*, 1967, 1057.
2 B. F. G. Johnson, R. D. Johnston and J. Lewis, *J. Chem. Soc. A*, 1968, 2865.
3 C. R. Eady, B. F. G. Johnson and J. Lewis, *J. Chem. Soc., Dalton Trans.*, 1975, 2606.
4 R. Mason and W. R. Robinson, *Chem. Commun.*, 1968, 468.
5 L. J. Farrugia, *Acta Crystallogr., Sect. C*, 1988, **44**, 997.
6 D. Braga, M. A. Gallop, F. Grepioni, B. F. G. Johnson, J. Lewis, M. Martinelli and E. Parisini, *J. Chem. Soc., Dalton Trans.*, 1992, 807.
7 D. Braga, M. A. Gallop, F. Grepioni, B. F. G. Johnson, J. Lewis and M. Martinelli, *J. Chem. Soc., Chem. Commun.*, 1990, 53.
8 S. Aime, M. T. Camellini, L. Milone, D. Osella, A. Tiripicchio, A. Vaglio and M. Valle, *Inorg. Chim. Acta*, 1979, **34**, 49.
9 D. Braga, H. Chen, F. Grepioni, B. F. G. Johnson, J. Lewis and E. Parisini, *J. Chem. Soc., Dalton Trans.*, 1991, 215.
10 P. J. Bailey, D. Braga, P. J. Dyson, F. Grepioni, B. F. G. Johnson, J. Lewis and P. Sabatino, *J. Chem. Soc., Chem. Commun.*, 1992, 177.
11 P. J. Bailey, D. Braga, P. J. Dyson, F. Grepioni, B. F. G. Johnson, J. Lewis, P. R. Raithby, P. Sabatino and D. Stalke, *J. Chem. Soc., Chem. Commun.*, 1993, 985.
12 M. P. Gomez-Sal, B. F. G. Johnson, J. Lewis, P. R. Raithby and A. H. Wright, *J. Chem. Soc., Chem. Commun.*, 1985, 1682.
13 D. Braga, F. Grepioni, B. F. G. Johnson, J. Lewis, M. Martinelli and A. H. Wright, *J. Chem. Soc., Chem. Commun.*, 1990, 364.
14 D. Braga, F. Grepioni, C. E. Housecroft, B. F. G. Johnson, J. Lewis and M. Martinelli, *Organometallics*, 1991, **10**, 1260.
15 See, for example, G. A. Somorjai, *J. Phys. Chem.*, 1990, **94**, 1013.

16 P. J. Bailey, D. Braga, P. J. Dyson, F. Grepioni, B. F. G. Johnson, J. Lewis and S. Righi, *Organometallics*, 1992, **11**, 4042.
17 R. Adams and W. Wu, *Polyhedron*, 1992, **11**, 2123.
18 P. J. Dyson, B. F. G. Johnson, J. Lewis, M. Martinelli, D. Braga and F. Grepioni, *J. Am. Chem. Soc.*, in the press.
19 A. Sirigu, M. Bianchi and E. Benedetti, *Chem. Commun.*, 1969, 596; D. Braga, F. Grepioni, P. J. Dyson, B. F. G. Johnson, P. Frediani, M. Bianchi and F. Piacenti, *J. Chem. Soc., Dalton Trans.*, 1992, 2565.
20 V. G. Albano, D. Braga and F. Grepioni, *Acta Crystallogr., Sect. B*, 1989, **45**, 60; D. Braga and F. Grepioni, *J. Organomet. Chem.*, 1987, **336**, C9; V. G. Albano and D. Braga, *Accurate Molecular Structures*, eds. A. Domenicano and I. Harghittay, Oxford University Press, 1991.
21 See, for example, D. Braga and F. Grepioni, *Organometallics*, 1991, **10**, 1254, 2563; 1992, **11**, 1256.
22 D. Braga, F. Grepioni, B. F. G. Johnson, Hong Chen and J. Lewis, *J. Chem. Soc., Dalton Trans.*, 1991, 2559.
23 W. Clegg, B. F. G. Johnson, J. Lewis, M. McPartlin, J. N. Nicholls, J. Puga, P. R. Raithby and M. J. Rosales, *J. Chem. Soc., Dalton Trans.*, 1983, 277.
24 M. A. Bennett and A. K. Smith, *J. Chem. Soc., Dalton Trans.*, 1974, 233.
25 *International Tables for X-Ray Crystallography*, Kynoch Press, Birmingham, 1974, vol. 4, pp. 99–149.
26 G. M. Sheldrick, SHELX 76, Program for Crystal Structure Determination, University of Cambridge, 1976.

Received 5th March 1993; *Paper* 3/01307C